# Apatite-forming ability of vinylphosphonic acid-based copolymer in simulated body fluid: effects of phosphate group content

# Apatite-forming ability of vinylphosphonic acid-based copolymer in simulated body fluid: effects of phosphate group content

Ryo Hamai[1], Yuki Shirosaki[2], Toshiki Miyazaki[1,*]

[1]Graduate School of Life Science and Systems Engineering, Kyushu Institute of Technology, Japan

[2]Frontier Research Academy for Young Researchers, Kyushu Institute of Technology, Japan

*Corresponding author

Toshiki Miyazaki

Graduate School of Life Science and Systems Engineering, Kyushu Institute of Technology, 2-4, Hibikino, Wakamatsu-ku, Kitakyushu 808-0196, Japan

Tel/Fax: +81-93-695-6025

E-mail: tmiya@life.kyutech.ac.jp

**Abstract**

Phosphate groups on materials surfaces are known to contribute to apatite formation upon exposure of the materials in simulated body fluid (SBF) and improved affinity of the materials for osteoblast-like cells. Typically, polymers containing phosphate groups are organic matrices consisting of apatite–polymer composites prepared by biomimetic process using SBF. $Ca^{2+}$ incorporation into the polymer accelerates apatite formation in SBF owing because of increase in the supersaturation degree, with respect to apatite in SBF, owing to $Ca^{2+}$ release from the polymer. However, the effects of phosphate content on the $Ca^{2+}$ release and apatite-forming abilities of copolymers in SBF are rather elusive. In this study, a phosphate-containing copolymer prepared from vinylphosphonic acid (VPA), 2-hydroxyethyl methacrylate (HEMA), and triethylene glycol dimethacrylate (TEGDMA) was examined. The release of $Ca^{2+}$ in Tris-NaCl buffer and SBF increased as the additive amount of VPA increased. However, apatite formation was suppressed as the phosphate groups content increased despite the enhanced release of $Ca^{2+}$ from the polymer. This phenomenon was reflected by changes in the surface zeta potential. Thus, it was concluded that the apatite-forming ability of VPA-HEMA-TGEDMA-$CaCl_2$ copolymer was governed by surface state rather than $Ca^{2+}$ release in SBF.

## 1. Introduction

Bone-bonding bioactive ceramics, such as Bioglass [1], glass-ceramics A-W [2], and sintered hydroxyapatite (HAp) [3], have been clinically employed as bone substitutes for repairing severe bone defects induced by accident or disease. When artificial materials are implanted in the affected bone area, the fibrous tissue encapsulates and isolates the materials surrounding the living bone. In contrast, bioactive ceramics can bond to living bone directly owing to their ability to form a bone-like apatite layer on their surface. However, bioactive ceramics have some drawbacks e.g., they cannot deform easily to fit into the defect area or they exert stress shielding effects after implantation. Such issues are due to the brittleness and high Young's modulus of ceramics.

As a result, organic–inorganic composites, for bone substitutes, have been examined to improve the mechanical properties of bioactive ceramics. The biomimetic process using simulated body fluid (SBF) is one of the methods commonly employed for preparing apatite–organic polymer composites. Such composites are expected to show mechanical properties similar to that of living bone as well as bioactivity. In this process, functional groups that can induce heterogeneous nucleation of apatite such as –COOH [4], $–SO_3H$ [5], $–PO_3H_2$ [4], Si–OH [6], Ti–OH [7], or Ta–OH [8] are introduced

into the organic matrix to obtain the composite.

The heterogeneous nucleation of apatite is promoted by the release of chemical species, thereby increasing the supersaturation degree with respect to apatite [9]. For example, to release $Ca^{2+}$ from the polymers, calcium salt [5, 10] is added or treatment with aqueous solutions of calcium salts [11–14] is performed. In the case of $CaCl_2$ treatment, polymers that feature excellent swelling properties in aqueous solution are used, thus facilitating the release of $Ca^{2+}$ to SBF [12].

Phosphate groups are effective for not only apatite formation, but also activity of osteoblast-like cells [15–16]. The cell adhesion and growth was increased as phosphate content increases. The incorporation of phosphate groups into the polymer is expected to afford various composites with high biological compatibility.

In our previous research, a phosphate-containing copolymer was prepared from vinylphosphonic acid (VPA) and triethylene glycol dimethacrylate (TEGDMA) through radical polymerization [17]. Although the low added amount of sodium *p*-toluene sulfonate (*p*-TSS), as a polymerization accelerator, inhibited degradation of the polymer, apatite was not formed in SBF irrespective of the composition employed. This phenomenon suggests that the presence of phosphate groups is insufficient to induce apatite formation.

Conversely, incorporating $Ca^{2+}$ could be effective for improving the apatite-forming ability of the copolymer. Moreover, the phosphate groups in the polymer are expected to influence the adsorption and release of $Ca^{2+}$ because phosphate is hydrophilic and can readily instigate ion–ion interactions with $Ca^{2+}$ [18].

Furthermore, phosphate content is also expected to affect heterogeneous nucleation of apatite on the copolymer in SBF due to the above mentioned ion-ion interaction. Increase in carboxyl group content promotes the heterogeneous nucleation thorough interaction with $Ca^{2+}$ [4]. Several researchers investigated apatite-forming ability of the synthetic polymer [19] or natural polymer [20] containing phoshonic acid through the phosphorylation process. However, these reports had no discussion regarding the effects of phosphate group content on surface condition and its apatite formation behavior in SBF. These points are important to obtain the apatite-phosphate polymer composites through the biomimetic process using SBF.

In this study, VPA-based copolymers having different phosphate contents were prepared by addition of 2-hydroxyethyl methacrylate (HEMA) and TEGDMA. Apatite formation on the copolymers in SBF was investigated and discussed in terms of $Ca^{2+}$ release, ionic interaction between the phosphate group and $Ca^{2+}$, and variation in the surface zeta potential.

## 2. Materials and methods

### 2.1. Preparation of VPA-HEMA-TEGDMA copolymers

Table 1 lists the amounts of monomers used for the preparation of the copolymers. The amount of the monomers totaled to 10 g. The specimens are denoted as *x*V*y*HzT, where *x*, *y*, and *z* refer to the amounts (mol%) of VPA (V), HEMA (H), and TEGDMA (T), respectively. Monomers VPA (95%, Tokyo Chemical Industry Co., Ltd., Tokyo, Japan), HEMA (95%, Wako Pure Chemical Industries, Ltd., Osaka, Japan), and TEGDMA (90%, Wako Pure Chemical Industries, Ltd.) were mixed. Then, 0.5 wt.% *p*-TSS (98%, Tokyo Chemical Industry Co., Ltd.) and 2 wt.% *N*,*N*′-dimethyl-*p*-toluidine (97%, Wako Pure Chemical Industries, Ltd.) were added to the combined monomers. Subsequently, (±)-camphorquinone (97%, Wako Pure Chemical Industries, Ltd.) was added at a concentration of 1 mol% relative to the total molar amount of monomers; the mixture was stirred in the dark for 1 h.

Then, the 1.1-g mixture was poured into polypropylene cups and irradiated under blue light (460 nm) for 1 h to polymerize the monomers. The obtained copolymer specimens were dried at 60°C for 1 day, and subsequently cut (10 mm × 10 mm × 1 mm) and polished with waterproof abrasive paper (SiC, #1000). The specimens were

then soaked in ultra pure water for 1 day at room temperature to remove unreacted reagents. Subsequently, the copolymer specimens were soaked in 30 mL of 1 kmol·m$^{-3}$ calcium chloride solution at 36.5°C for 1 day.

## 2.2. Soaking of specimens in SBF and Tris-NaCl buffer solutions

The copolymers specimens were soaked in 30 cm$^3$ SBF at 36.5°C for various times up to 5 days. SBF ($Na^+$ 142.0, $K^+$ 5.0, $Mg^{2+}$ 1.5, $Ca^{2+}$ 2.5, $Cl^-$ 147.8, $HCO_3^-$ 4.2, $HPO_4^{2-}$ 1.0, $SO_4^{2-}$ 0.5 mol·m$^{-3}$) was prepared by adding NaCl, $NaHCO_3$, KCl, $K_2HPO_4 \cdot 3H_2O$, $MgCl_2 \cdot 6H_2O$, $CaCl_2$, and $Na_2SO_4$ (Nacalai Tesque, Inc., Kyoto, Japan) to ultra pure water in this order [6]. The pH of the resulting solution was adjusted to 7.40 by addition of tris(hydroxymethyl)aminomethane (Nacalai Tesque, Inc.) and an appropriate volume of 1 kmol m$^{-3}$ HCl solution.

Also, the specimens were soaked in 30 cm$^3$ Tris-NaCl buffer at 36.5°C for 1 day to measure the amount of $Ca^{2+}$ released from the copolymer specimens. Tris-NaCl buffer (142 mol·m$^{-3}$ NaCl and 50 mol·m$^{-3}$ tris(hydroxymethyl)aminomethane) was prepared by sequential addition of NaCl and tris(hydroxymethyl)aminomethane to ultra pure water. Then, an appropriate volume of 1 kmol·m$^{-3}$ HCl solution was added to the solution to adjust the pH to 7.40.

## 2.3. Characterization

Following soaking of the copolymer specimens in $CaCl_2$ solution, the specimens were analyzed by wavelength-dispersive X-ray fluorescence spectroscopy (ZSX101e, Rigaku Co., Tokyo, Japan) to determine the Ca content. The surface of the copolymer specimens soaked in SBF for various periods was analyzed with thin-film X-ray diffraction (TF-XRD; MXP3V, Mac Science, Co., Yokohama, Japan), scanning electron microscopy (SEM) using an S-3500N scanning electron microscope (Hitachi Co., Tokyo, Japan) equipped with an energy-dispersive X-ray (EDX) analysis system (EMAX Energy, Horiba Ltd., Kyoto, Japan), and Fourier transform infrared (FT-IR; FT/IR-6100, JASCO Co., Tokyo, Japan) spectroscopy using an attenuated total reflectance method. In the TF-XRD analysis, the angle of the X-ray (Cu Kα) was fixed at 1° relative to the surface of the sample. For the SEM-EDX analysis, the surfaces of the samples were coated with carbon using a carbon coater (CADE, Meiwafosis Co., Ltd., Osaka, Japan). For the FT-IR analysis, a diamond prism was used to record the FT-IR spectra at a resolution of 1 $cm^{-1}$.

The concentrations of Ca in the Tris-NaCl buffer and P and Ca in SBF after soaking the copolymer specimens were measured using inductively coupled plasma

optical emission spectrometry (Optima 4300DV CYCLON, PerkinElmer Inc., London, UK). The pH of the SBF solution following soaking of the different specimens was determined using a pH meter (F-23IIC, Horiba Ltd.).

The surface zeta potential of the copolymer specimens in SBF was measured using a zeta potential analyzer (Otsuka Electronics Co., Osaka, Japan) connected to box-like quartz cell. After the copolymer specimens were soaked in SBF for various periods, the surface of the specimens was washed with ultra pure water. The washed specimen was introduced into the quartz cell. Then, fresh SBF and polyethylene latex particles (Otsuka Electronics Co.) were injected into the cell. To measure the surface zeta potential, the electrophoretic mobility of the particles was measured using the laser Doppler method.

## 3. Results

Figure 1a shows the content of Ca in the specimens prepared with varying amounts of VPA after soaking in $CaCl_2$ solution. The content increased as the VPA/HEMA ratio increased. The Ca concentration in Tris-NaCl buffer after soaking the specimens for 1 day is shown in Fig. 1b. The concentration increased with increasing VPA/HEMA contents.

Figure 2 shows SEM images of the specimens after soaking in SBF for various periods. The deposition was observed on the surface of 01V94H05T after soaking SBF within 1 day. The morphology of deposition consisted of flake-like particles. On the other hand, deposition was not formed on the 10V85H05T and 40V85H05T within 5 days.

Figure 3 shows the TF-XRD patterns of the specimens after soaking in SBF for various periods. After soaking for 1 day, 01V94H05T displayed two broad peaks at $2\theta$ 26° and 32°, which were assigned to apatite (JCPDS #09-0432). In contrast, these peaks were not observed in 10V85H05T and 40V55H05T regardless of the soaking time.

Figure 4 shows the variations in the concentration of P and Ca in SBF and solution pH after soaking the specimens for various periods. As observed in Fig. 3a, for 01V94H05T, the concentration of P decreased with increasing soaking times. In contrast, the concentration of P remained rather constant after soaking 10V85H05T or 40V55H05T. Conversely, for all three specimens, the concentration of Ca initially increased and then decreased slightly with increasing soaking times (Fig. 4c, d). The concentration of Ca increased in the order of 01V94H05T < 10V85H05T < 40V55H05T. The solution pH, after soaking, decreased monotonically for 40V55H05T, whereas that of the remaining specimens initially increased slightly and subsequently remained

unchanged (Fig. 4b).

Figure 5 shows the changes in the molar ratio of Ca/P and content of P on the surfaces of 01V94H05T and 10V85H05T, and SEM images of 01V94H05T after soaking in SBF for various periods analyzed by SEM-EDX. The Ca/P ratio for both specimens decreased in the first 3 h of soaking and then increased. The Ca/P ratio of 01V94H05T was higher than that of 10V85H05T irrespective of soaking time. The P content of 01V94H05T increased after 6 h of soaking, whereas that of 10V85H05T remained constant at all soaking times studied. Deposition was first observed after 12 h on the surface of 01V94H05T in SBF.

Figure 6 shows the changes in the zeta potential of 01V94H05T and 10V85H05T. The potential of 01V94H05T changed from negative to positive after soaking in SBF for 9 h. In contrast, the potential of 10V85H05T only increased slightly from the negative value to attain a zero value after 6 h of soaking.

Figure 7 shows the FT-IR spectra of 01V94H05T and 10V85H05T after soaking in SBF for various periods. The peak at 900 $cm^{-1}$, which was attributed to C–C stretching vibrations of HEMA, was observed for 01V94H05T after soaking in SBF for 0–9 h [21-22]. The peak disappeared after 12 h of soaking owing to the formation of a deposition layer on the specimen. In contrast, 10V85H05 displayed a peak at 889 $cm^{-1}$,

which was attributed to P–O bond in the $–P–O^{-}\cdots Ca^{2+}$ complex, as well as the peak corresponding to C–C stretching at all soaking times investigated [17, 19].

## 4. Discussion

The amount of Ca incorporated into the prepared copolymer and released into Tris-NaCl increased with increasing contents of the phosphate group (Fig. 1). The swelling property of the copolymer is affected by not only the cross-link density, but also the charge of the functional groups [16, 23]. The repulsion induced by ionic groups with the same charge acts as a driving force for swelling. The increase in the phosphate group content enhances swelling, therefore higher contents of phosphate would promote the adsorption of $Ca^{2+}$ onto the copolymer upon $CaCl_2$ treatment and release of $Ca^{2+}$ into the solution.

Apatite formation on the copolymer was rather suppressed upon increases in the phosphate content despite the enhanced release of $Ca^{2+}$ from the copolymer. To further understand this phenomenon, the supersaturation degree with respect to apatite in SBF was calculated. Figure 8 shows changes in the relative supersaturation degree, $\sigma$, of the copolymers in SBF, calculated using Equation (1) [24]:

$$\sigma = \frac{IP_{HAp}^{\ 1/\nu} - Ksp_{HAp}^{\ 1/\nu}}{Ksp_{HAp}^{\ 1/\nu}}, \quad (1)$$

where $IP_{HAp}$, $Ksp_{HAp}$, and $\nu$ are the ionic activity products of HAp, solubility product of HAp ($5.5 \times 10^{-118}$), and the number of ions in an HAp molecule (18), respectively. The $IP_{HAp}$ was estimated according to Equation (2):

$$IP_{HAp} = (\gamma_{Ca^{2+}})^{10}(\gamma_{PO_4^{3-}})^{6}(\gamma_{OH^-})^{2}[Ca^{2+}]^{10}[PO_4^{\ 3-}]^{6}[OH^-]^{2}. \quad (2)$$

The values of $\gamma_{Ca^{2+}}$, $\gamma_{PO_4^{3-}}$, and $\gamma_{OH^-}$ are respectively 0.36, 0.06, and 0.72 at physiological ionic strength ($\mu$ = 0.16) [25]. For all the specimens, the degree of supersaturation increased slightly and subsequently decreased. The degree of supersaturation increased in the order of 40V55H05T ≈ 01V94H05T < 10V85H05T. However, apatite was only observed on 01V94H05T (Fig. 2 and 3). These results suggest that apatite formation of the copolymer was governed by surface chemical state rather than increase in supersaturation degree owing to $Ca^{2+}$ release.

The difference in the surface state of the specimens having various contents of phosphate in SBF can be interpreted as follows. The zeta potential of 01V94H05T increased more significantly than that of 10V85H05T after 6 h of soaking in SBF (Fig. 6). As reported, the potential of soft solids, such as a gel or a polymer, is governed by not only the charge on the outermost surface, but also the charge inside the solid, unlike that of hard solids such as metal oxides [26–27]. Therefore, $Ca^{2+}$ would accumulate near

the surface of the soft specimens after soaking in SBF. Furthermore, the complex –P–$O^{-}\cdots Ca^{2+}$ formed on 10V85H05T only upon soaking in SBF (Fig. 7). Based on the result, it is assumed that the amount of free $Ca^{2+}$ is larger than that of $Ca^{2+}$ tightly bound to phosphate groups on the surface and/or inside 01V94H05T and that the negative charge on 10V85H05T is neutralized in SBF upon tight binding with $Ca^{2+}$. The free $Ca^{2+}$ would readily bond with phosphate ions in SBF for conversion into apatite. The decrease in the zeta potential of 01V94H05T after 9 h of soaking supports this assumption. Conversely, further ion adsorption to induce apatite nucleation did not occur on 10V85H05T.

The surface potential has been previously reported as a contributing factor to the formation of apatite on various substrates in SBF [28]. For example, the zeta potential of high-molecular-weight polyethylene containing $–SO_3H$ groups and $Ca^{2+}$ becomes positive upon soaking in SBF and subsequently adsorbs $PO_4^{3-}$ to induce apatite nucleation [29]. In contrast, the polymer modified with $–SO_3H$ only did not form apatite in SBF. Accordingly, as observed, the surface potential of 10V85H05T was insufficiently positive to adsorb $PO_4^{3-}$ and therefore it did not form apatite.

The results in this study showed that materials with larger amounts of phosphate group inhibit apatite formation in SBF. However, as reported, phosphate

groups in the self-assembled monolayer on gold can interact with $PO_4^{3-}$ after binding with $Ca^{2+}$ in SBF, subsequently instigating apatite formation [4]. This suggests that the binding state of the phosphate groups with $Ca^{2+}$ is different in the present results. Specifically, the acidity of the phosphate-containing compounds is different owing to their different chemical structure [30]. The effects of chemical structure and space distribution of phosphate groups on the binding state and apatite formation on phosphate-containing polymers deserve further investigation in future work.

## 5. Conclusion

The effect of the amount of phosphate groups on the apatite-forming ability of VPA-HEMA-TEGDMA treated with $CaCl_2$ solution was investigated in SBF. Increasing the content of VPA enhanced the release of $Ca^{2+}$ from copolymer. However, apatite formation was only induced on the copolymer prepared with 1 mol% of VPA (lowest amount studied). Higher VPA content rather inhibited the apatite formation because $PO_4^{3-}$ could not react with free $Ca^{2+}$ on the surface due to the increase in amount of $Ca^{2+}$ tightly binding with phosphate group. It was found that phosphate groups in VPA produce the unsuitable surface condition for heterogeneous nucleation of the apatite. The future works are required to precisely investigate the effects of detailed chemical

structure and binding state with $Ca^{2+}$ of the phosphate groups on apatite formation.

## References


[1] Hench LL. Bioceramics. J Am Ceram Soc. 1998;81:1705-8.

[2] Kokubo T, Kim HM, Kawashita M. Novel bioactive materials with different mechanical properties. Biomaterials. 2003;24:2161-2175.

[3] Jarcho M, Bolen CH, Thomas MB, Bobick J, Kay JF, Doremus RH. Hydroxyapatite synthesis and characterization in dense polycrystalline forms. J Mater Sci, 1976;11: 2027–2035.

[4] Tanahashi M, Matsuda T. Surface functional group dependence on apatite formation on self-assembled monolayers in a simulated body fluid. J Biomed Mater Res 1997;34:305-315.

[5] Kawai T, Ohtsuki C, Kamitakahara M, Miyazaki T, Tanihara M, Sakaguchi Y, Konagaya S. Coating of an appetite layer on polyamide films containing sulfonic groups by a biomimetic process. Biomaterials 2004;25:4529-4534.

[6] Cho SB, Nakanishi K, Kokubo T, Soga N, Kamamura T, Kitsugi T, Yamamuro T. Dependence of apatite formation on silica gel on its Structure: effect of heat treatment. J Am Ceram Soc 1995;78:1769-1774.

[7] Uchida M, Kim HM, Fujibayashi S, Nakamura T. Structural dependence of apatite formation on titania gels in a simulated body fluid. J Biomed Mater Res A, 2003;64A:164-170.

[8] Miyazaki T, Kim HM, Kokubo T, Kato H, Nakamura T. Induction and acceleration of bonelike apatite formation on tantalum oxide gel in simulated body fluid. J Sol-Gel Sci Tech 2001;21:83-88.

[9] Ohtsuki C, Kokubo T, Yamamuro T, Mechanism of apatite formation on $CaO-SiO_2-P_2O_5$ glass in a simulated body fluid. J Non-Cryst Solids, 1992;143:84-92.

[10] Miyazaki T, Ohtsuki C, Akioka Y, Tanihara M, Nakao J, Sakaguchi Y, Konagaya S. Apatite deposition on polyamide films containing carboxyl group in a biomimetic solution. J Mater Sci Mater Med. 2003;14:569-74.

[11] Takeuchi A, Ohtsuki C, Miyazaki T, Tanaka H, Yamazaki M, Tanihara M. Deposition of bone-like apatite on silk fiber in a solution that mimics extracellular fluid. J Biomed Mater Res A, 2003;65A:283-189.

[12] Nakata R, Miyazaki T, Morita Y, Ishida E, Iwatsuki R, Ohtsuki C. Apatite formation abilities of various carrageenan gels in simulated body environment. J Ceram Soc Japan 2010;118:487-490.

[13] Kawashita M, Nakao M, Minoda M, Kim HM, Beppu T, Miyamoto T, Kokubo T,

Nakamura T. Apatite-forming ability of carboxyl group-containing polymer gels in a simulated body fluid. Biomaterials 2003;24:2477-2484.

[14] Leonor IB, Kim HM, Balas F, Kawashita M, Reis RL, Kokubo T, Nakamura T, Functionalization of different polymers with sulfonic groups as a way to coat them with a biomimetic apatite layer. J Mater Sci Mater Med 2007;18:1923-1930.

[15] Gemeinhart RA, Bare CM, Haasch RT, Gemeinhart EJ. Osteoblast-like cell attachment to and calcification of novel phosphate-containing polymeric substrate. J Biomed Mater Res A 2006;78A:433-440.

[16] Tan J, Gemeinhart RA, Ma M, Saltzman WM, Improved cell adhesion and proliferation on synthetic acid-containing hydrogel. Biomaterials 2005;26:3663-3671.

[17] Hamai R, Shirosaki Y, Miyazaki T. Biomineralization behavior of a vinylphosphonic acid-based copolymer added with polymerization accelerator in simulated body fluid. J Asian Ceram Soc 2015;3:407-411.

[18] Ellis J, Anstice M, Wilson AD. The glass polyphosphonate cement: A novel glass-ionomer cement based on poly(vinyl phosphonic acid). Clin Mater 1991;7:341-346.

[19] Jin S, Gonsalves E. Functionalized copolymers and their composites with polylactide and hydroxyapatite. J Mater Sci Mater Med 1999;10:363-368.

[20] Yin YJ, Luo XY, Cui JF, Wang CY, Guo XM, Yao KD. A study on biomineralization Behavior of N-methylene phosphochitosan scaffolds. Macromol Biosci 2004:4:971-977.

[21] Ferreira L, Vidal MM, Gil MH. Evaluation of poly(2-hydroxyethyl methacrylate) gels as drug delivery systems at different pH values. Int J Pharm 2000;194:169–180.

[22] Faria MDG, Dias JJCT, Fausto R. Conformation stability for methyl acrylate: a vibrational spectroscopic ab initio MO study. Vib. Spectr 1991:2:43-60.

[23] Garrett Q, Laycock B, Garrett RW. Hydrogel lens monomer constituents modulate protein sorption. Invest Ophthalmol Vis Sci 2000;41:1687-1695.

[24] Hata K, Kokubo T, Nakamura T, Yamamuro T. Growth of a Bonelike Apatite Layer on a Substrate by a Biomimetic Process. J Am Ceram Soc 1995;78:1049-1053.

[25] Neuman W, Neuman M. The chemical dynamics of bone mineral. Chicago: University of Chicago Press; 1958.

[26] Ohshima H, Makino K, Kondo T. Interfacial electric phenomena and Donnan potential in membranes. Membrane 1987;12:425-430.

[27] Makino K, Ohshima H, Kondo T. Surface potential an ion-penetrable charged membrane. J Theor Biol 1987;125:367-368.

[28] Kim HM, Himeno T, Kawashita M, Lee JH, Kokubo T, Nakamura T. Surface

potential change in bioactive titanium metal during the process of apatite formation in simulated body fluid. J Biomed Mater Res A, 2003;67A:1305-1309.

[29] Leonor IB, Kim HM, Balas F, Kawashita M, Reis RL, Kokubo T, Nakamura T. Surface potential change in bioactive polymer during the process of biomimetic apatite formation in a simulated body fluid. J Mater Chem 2007;17:4057-4063.

[30] MoszernM, Salz U, Zimmermann J. Chemical aspects of self-etching enamel–dentin adhesives: A systematic review. Dent Mater 2005;21:895-910.

## Figure and table captions

**Fig. 1** (a) Ca content in the copolymer specimens after soaking in 1 kmol $m^{-3}$ $CaCl_2$ solution and (b) Ca concentration in Tris-NaCl buffer following soaking of the different copolymer specimens ($N$ = 3).

**Fig. 2** SEM images of the specimens after soaking in SBF for various periods.

**Fig. 3** TF-XRD patterns of the copolymer specimens following soaking in SBF for various periods

**Fig. 4** Changes in (a) P concentration, (b) pH, and (c, d) Ca concentration in SBF following soaking of the different copolymer specimens ($N$ = 3).

**Fig. 5** Changes in the (a) molar ratio of Ca/P and (b) abundance of P on the surface of 01V94H05T and 10V85H05T following soaking in SBF

**Fig. 6** Changes in the surface zeta potentials of 01V94H05T and 10V85H05T following soaking in SBF ($N$ = 3).

**Fig. 7** FT-IR spectra of 01V94H05T and 10V85H05T following soaking in SBF for various periods

**Fig. 8** Changes in the relative supersaturation degree in SBF following soaking of the different copolymer specimens

**Table 1** Composition of the monomers employed during synthesis of the copolymer specimens

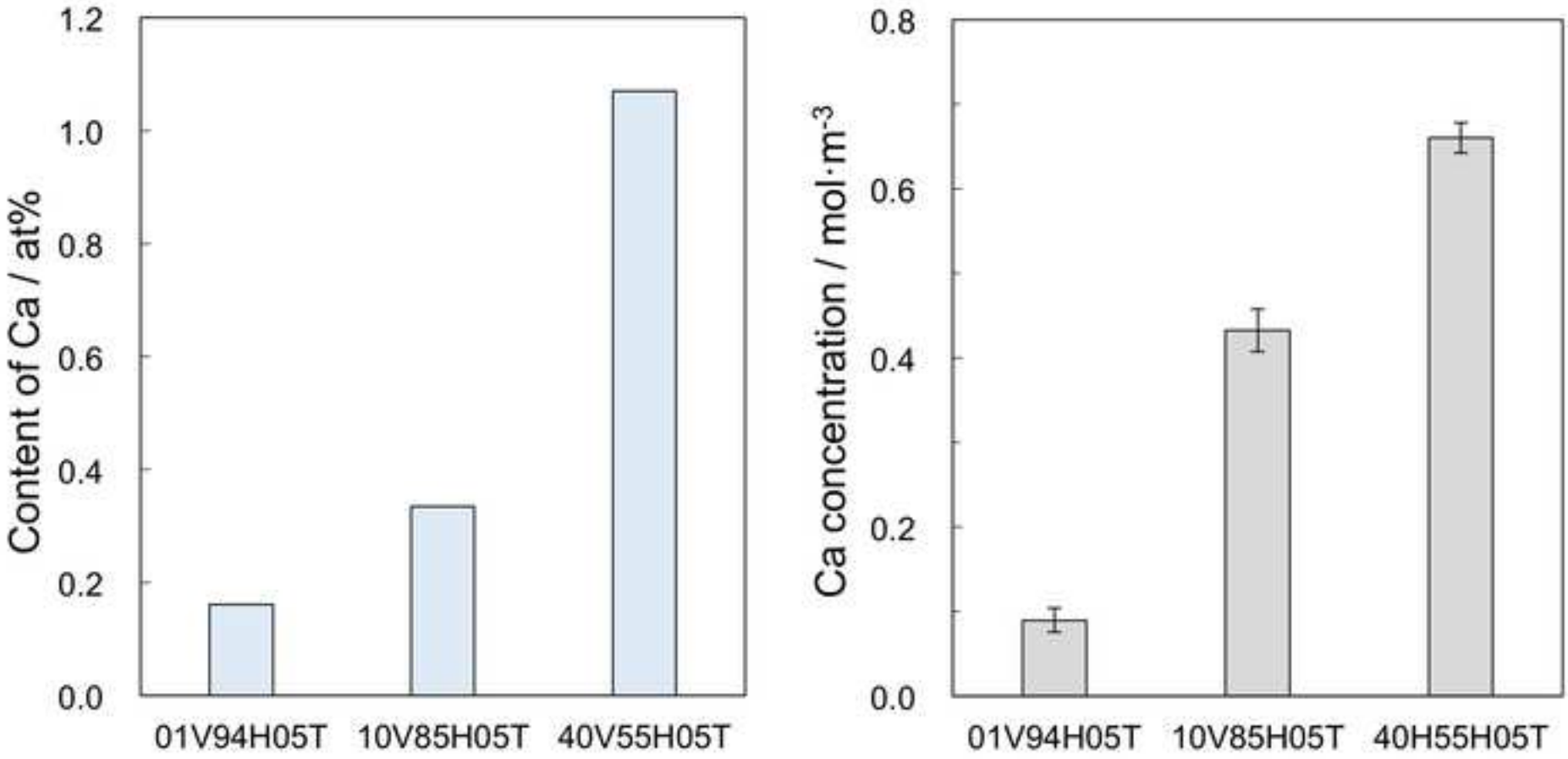


Fig. 1

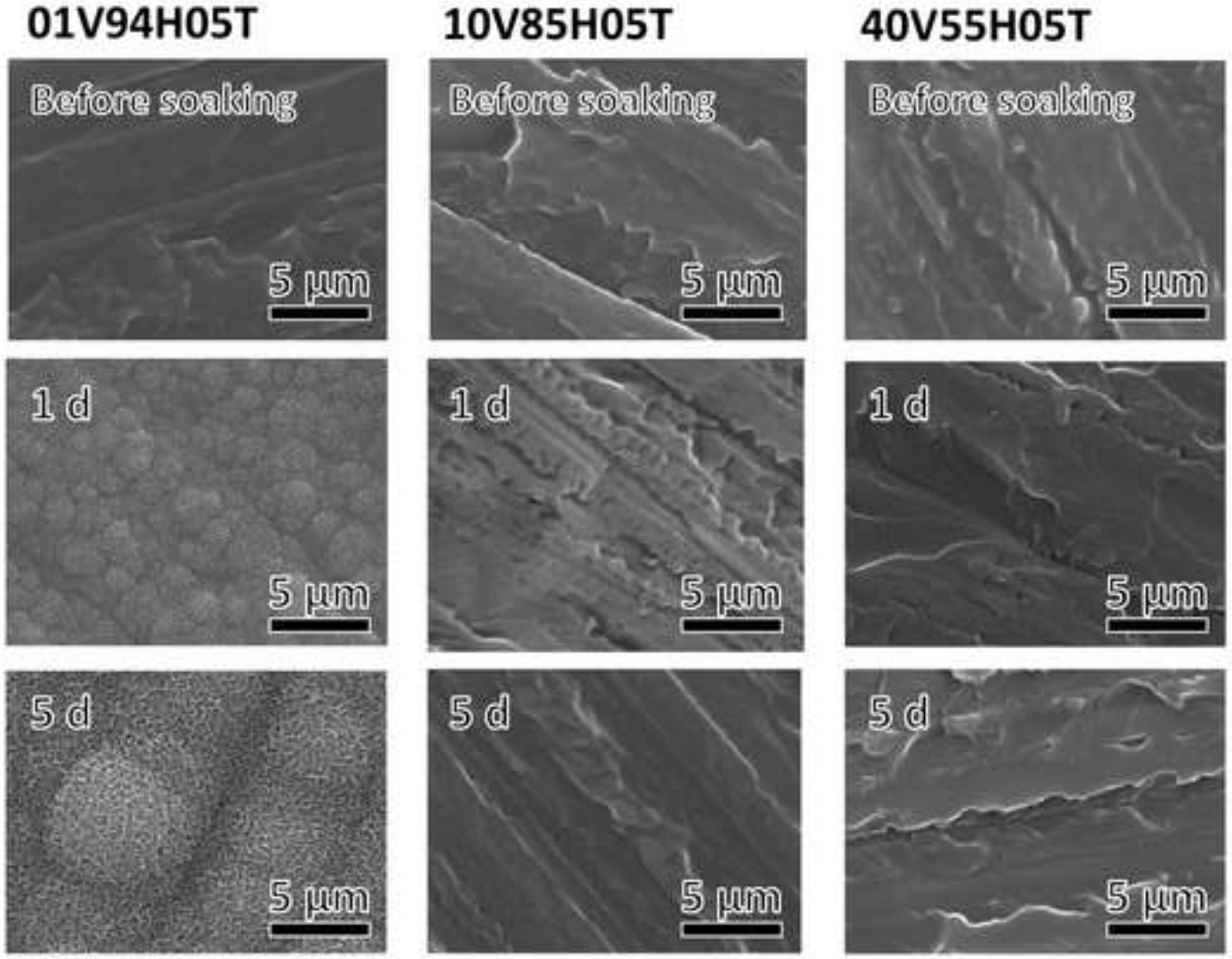


Fig. 2

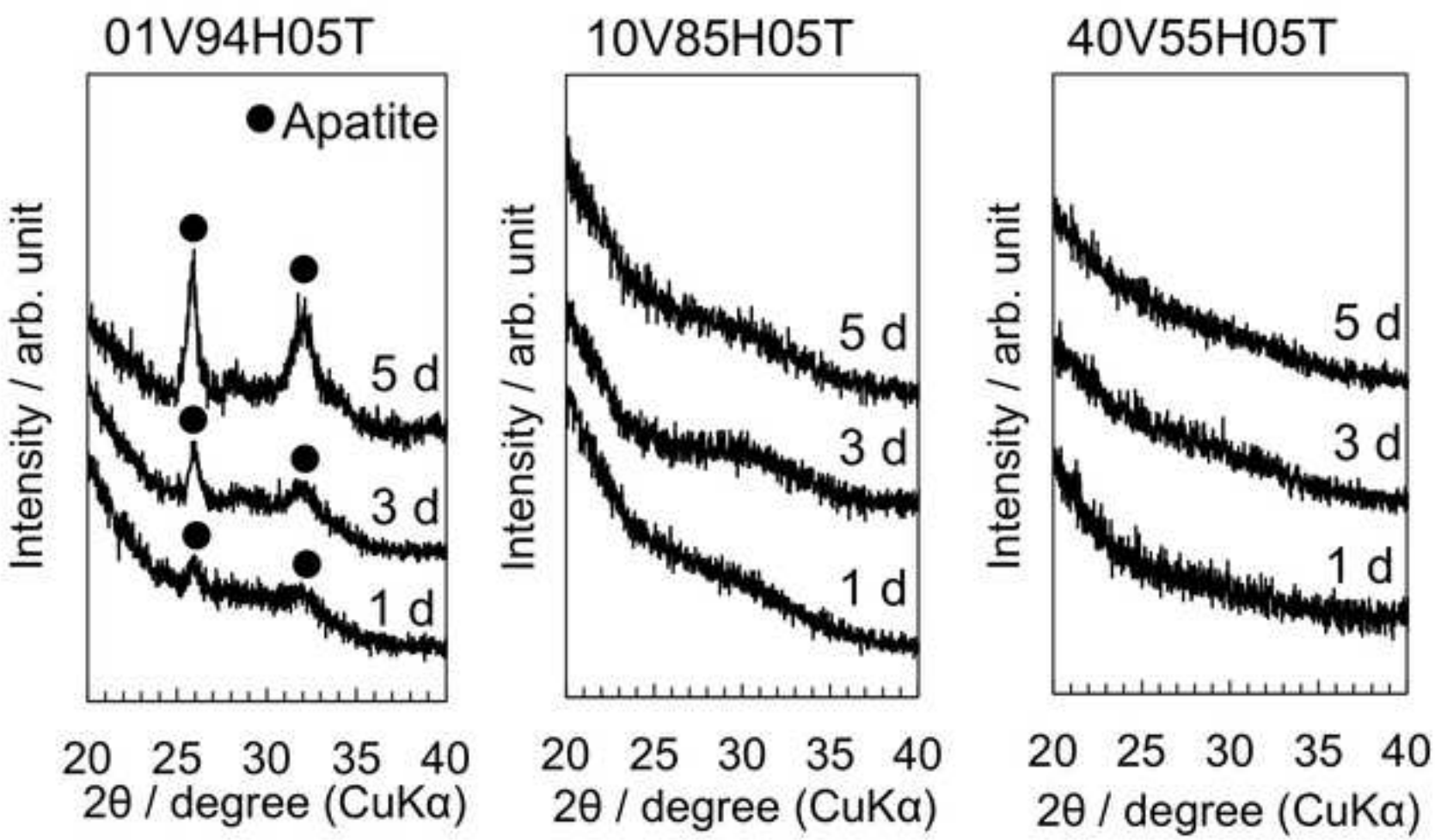


Fig. 3

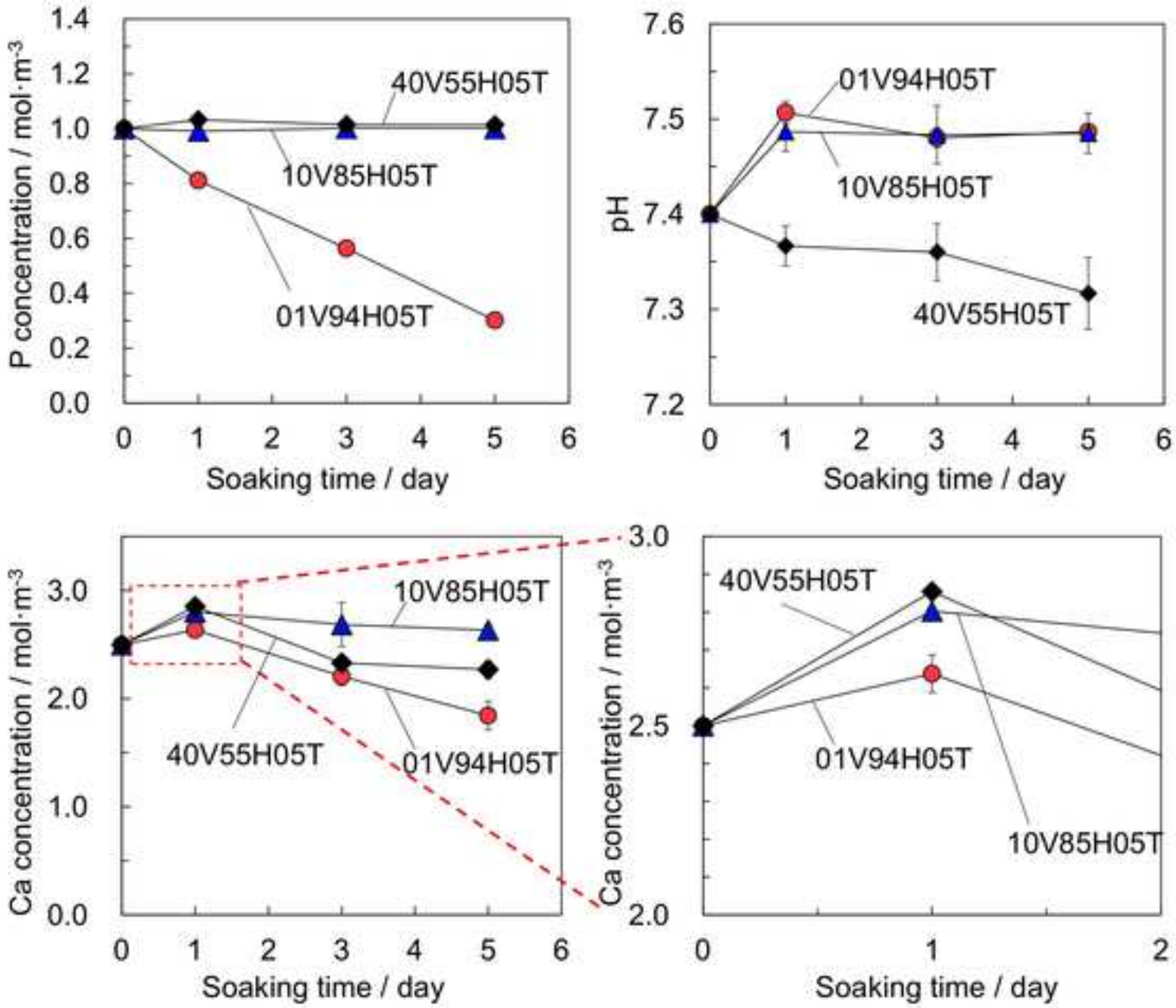


Fig. 4

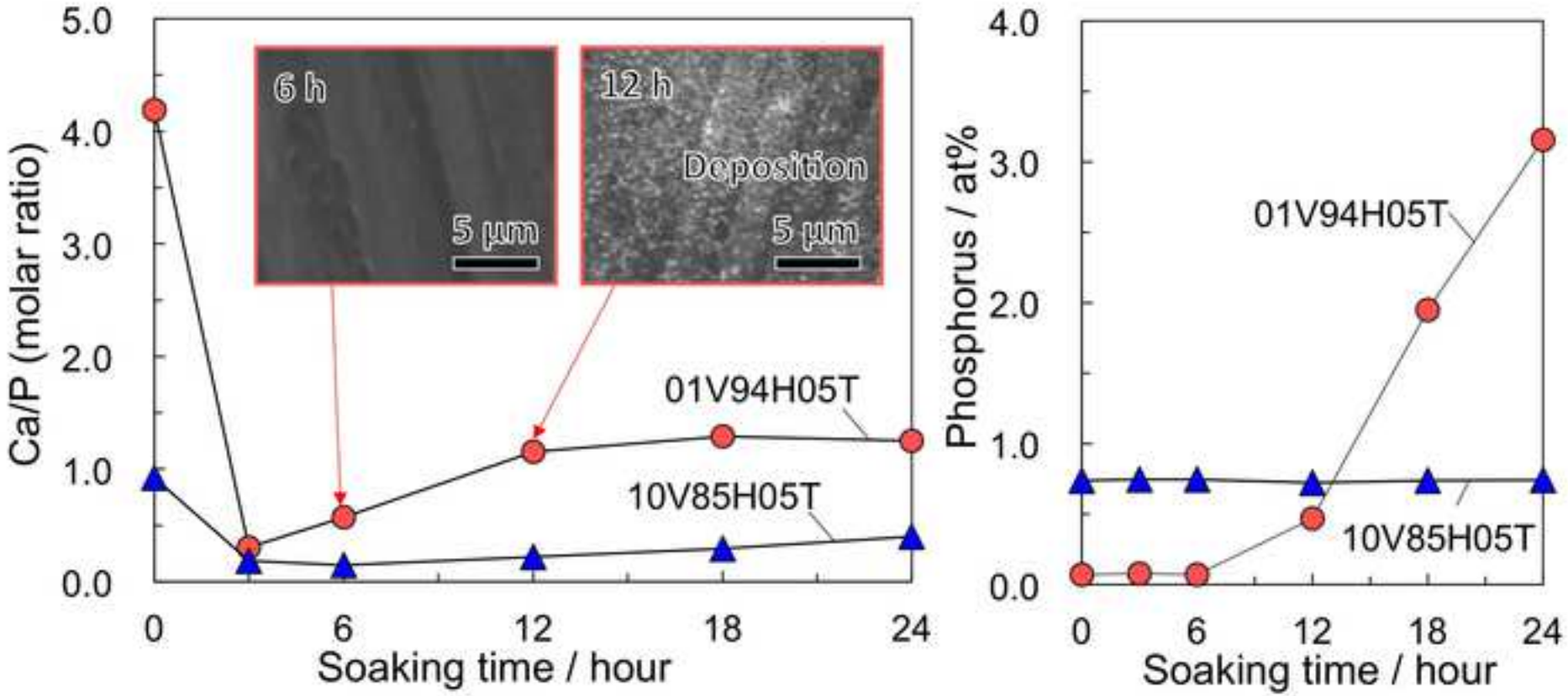


Fig. 5

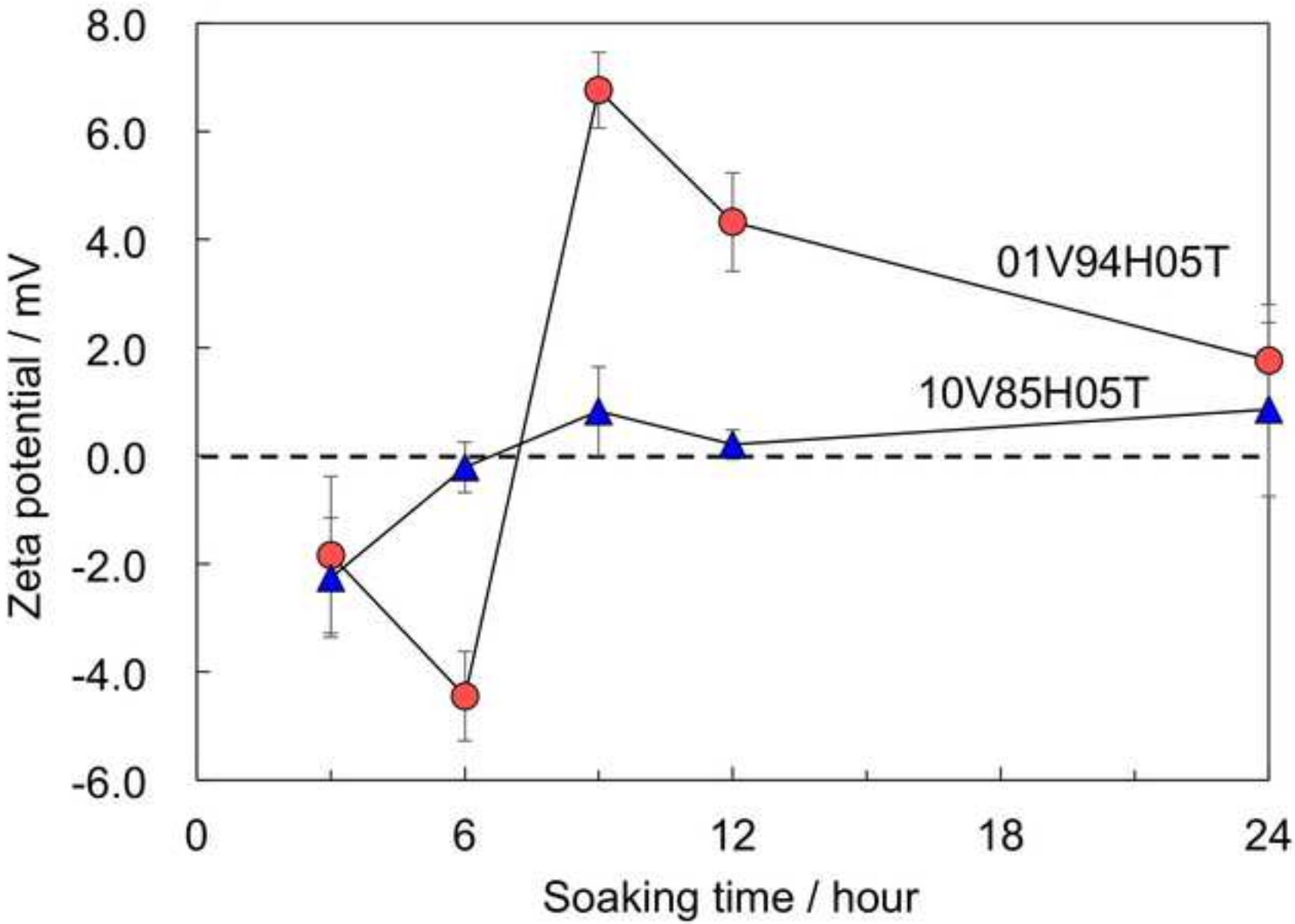


Fig. 6

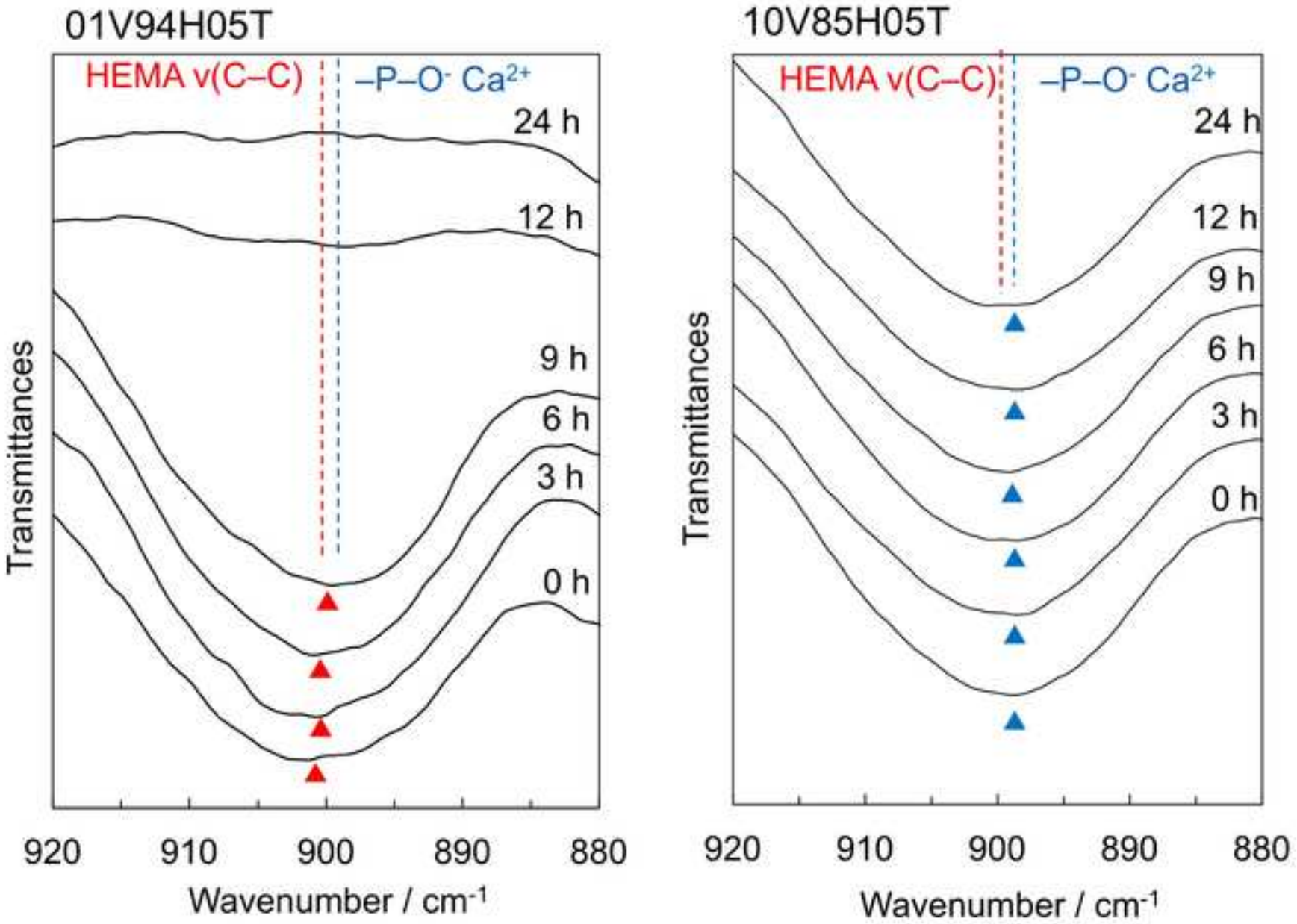


Fig. 7

Figure8



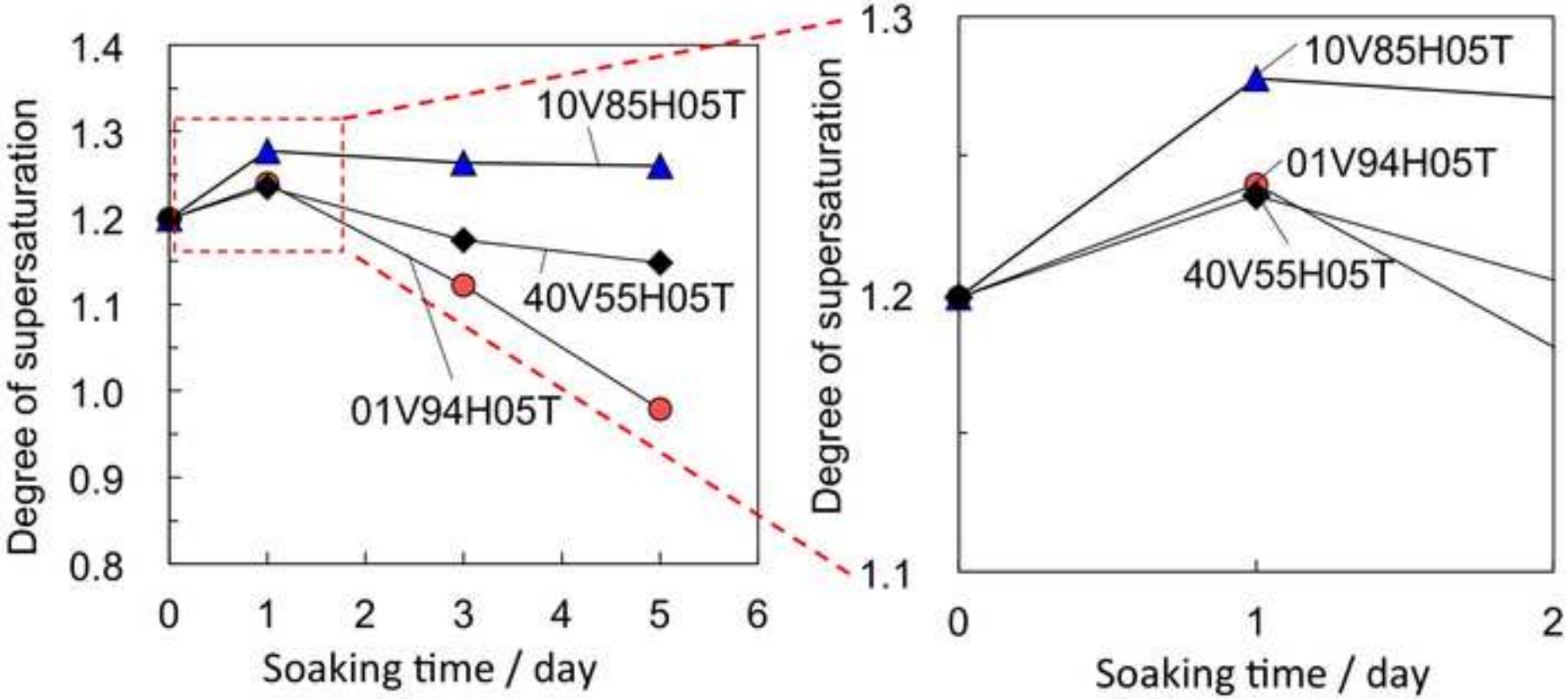


Fig. 8

Table 1

| Specimen | VPA /mol% | HEMA / mol% | TEGDMA / mol% |
|---|---|---|---|
| 40V55H05T | 40 | 55 | 5 |
| 10V85H05T | 10 | 85 | 5 |
| 01V94H05T | 1 | 94 | 5 |